Spatially Variant Resolution Modelling for Iterative List-Mode PET Reconstruction

Matthew Bickell, Lin Zhou, Johan Nuyts

Medical Imaging Research Centre

KULeuven, Belgium

KATHOLIEKE UNIVERSITEIT LEUVEN

Resolution modelling

Accurate system modelling can improve resolution

In MLEM:

1. The forward projection simulates a measurement process
2. The resulting projection is compared to the measured data
3. The result is backprojected and used as an update

Resolution modelling

A standard approach with MLEM:

Convolve the image with a Gaussian

- before forward projection, and
- after backprojection

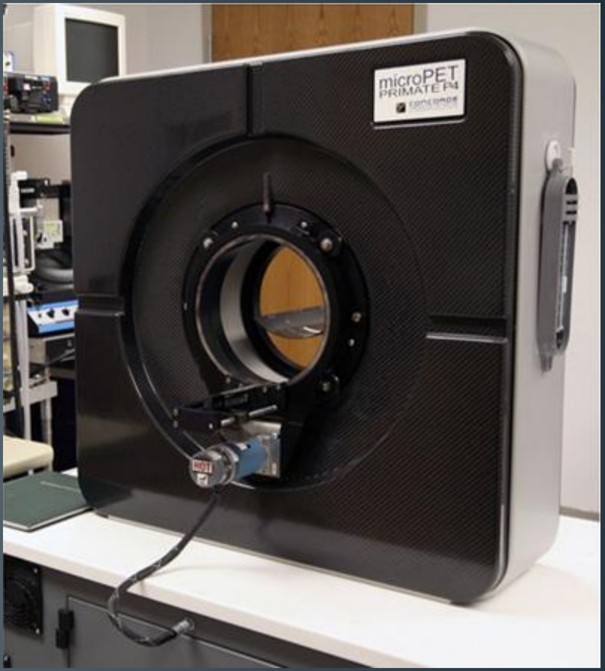

microPET FOCUS-220

Gaussian FWHM = 1.3 mm[1]

[1] Tai, Y., *et al*, "Performance evaluation of the microPET focus: a third-generation microPET scanner dedicated to animal imaging.", *J. Nucl. Med., 46:3, 2005*

The measurement process

Positron range

Photon acollinearity

Detector response

Inter-crystal scatter

Crystal crosstalk

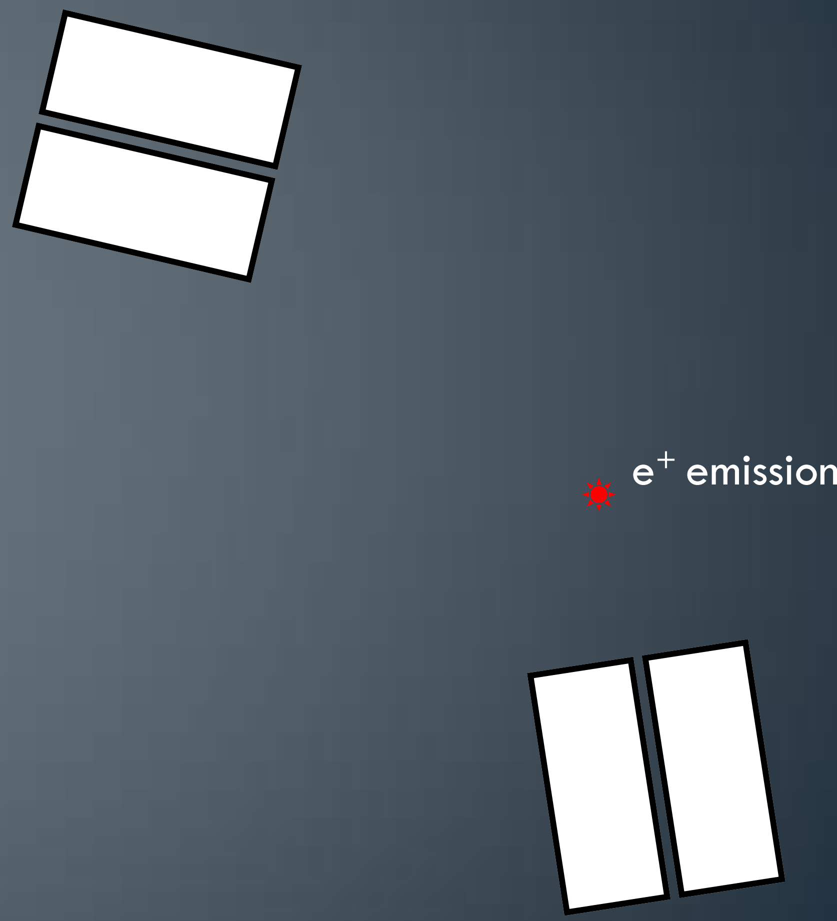

The measurement process

Positron range

Photon acollinearity

Detector response

Inter-crystal scatter

Crystal crosstalk

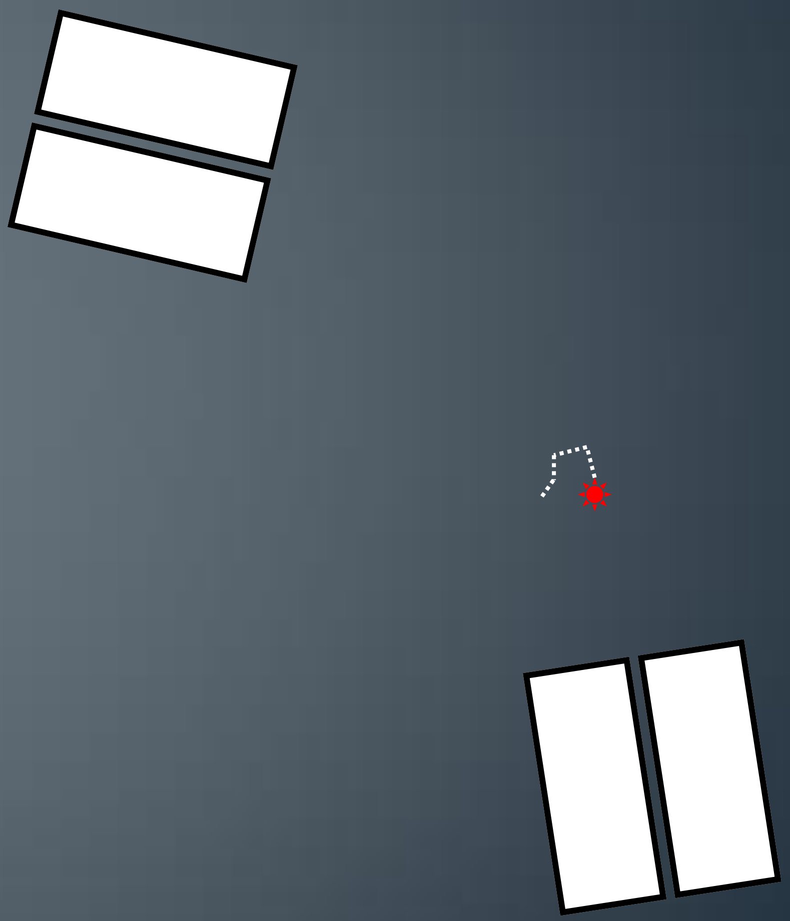

The measurement process

Positron range

Photon acollinearity

Detector response

Inter-crystal scatter

Crystal crosstalk

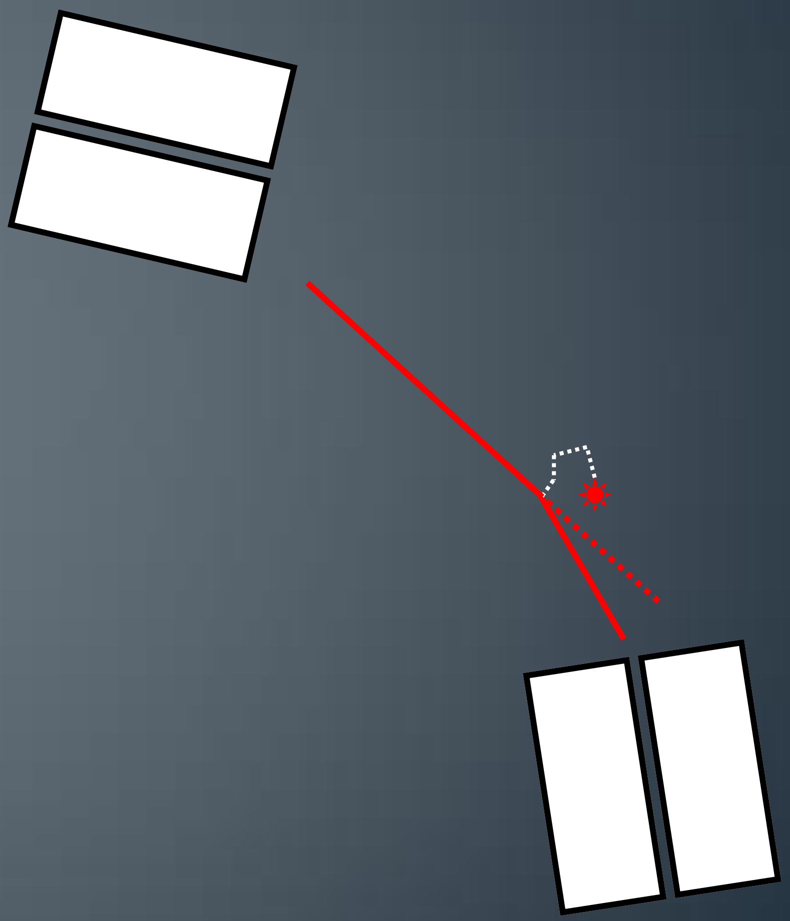

The measurement process

Positron range

Photon acollinearity

Detector response

Inter-crystal scatter

Crystal crosstalk

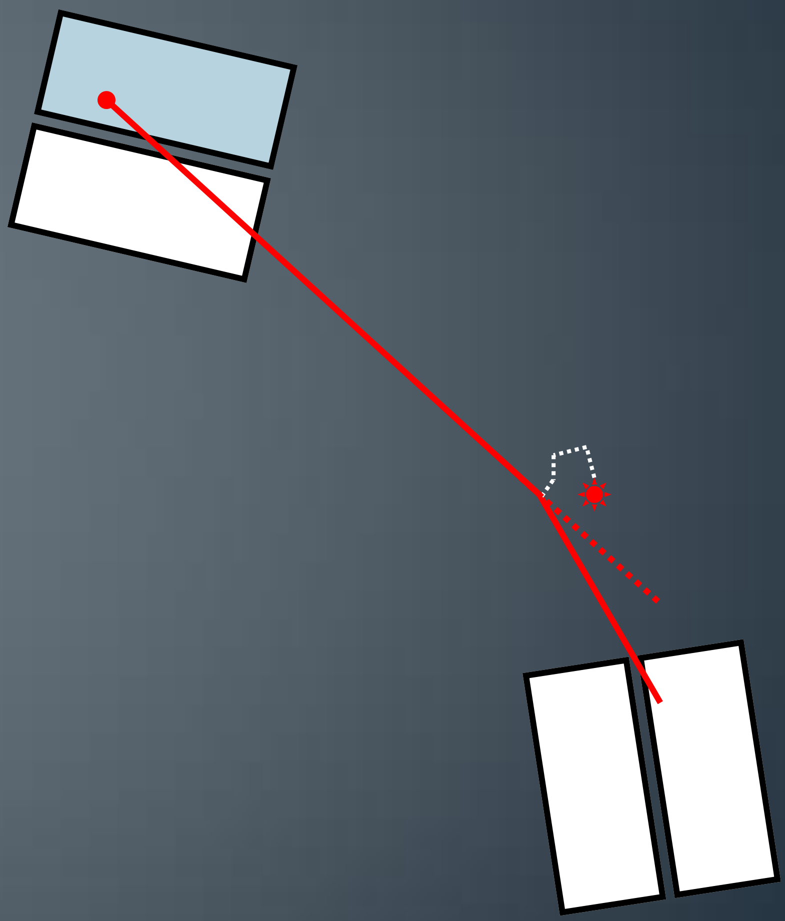

The measurement process

Positron range

Photon acollinearity

Detector response

Inter-crystal scatter

Crystal crosstalk

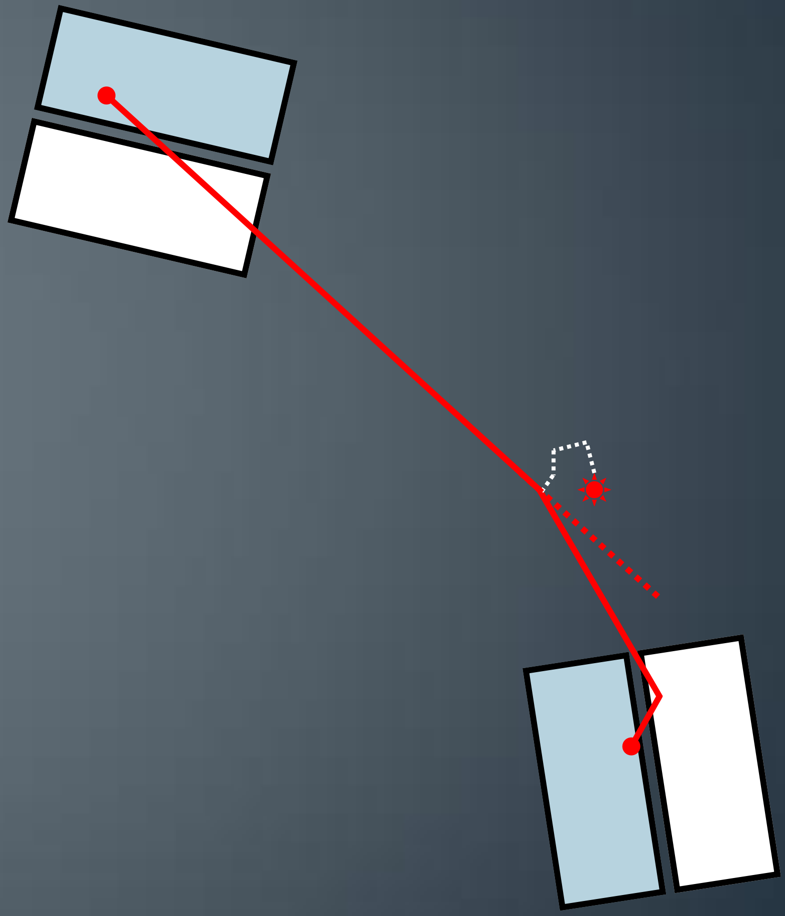

The measurement process

Positron range

Photon acollinearity

Detector response

Inter-crystal scatter

Crystal crosstalk

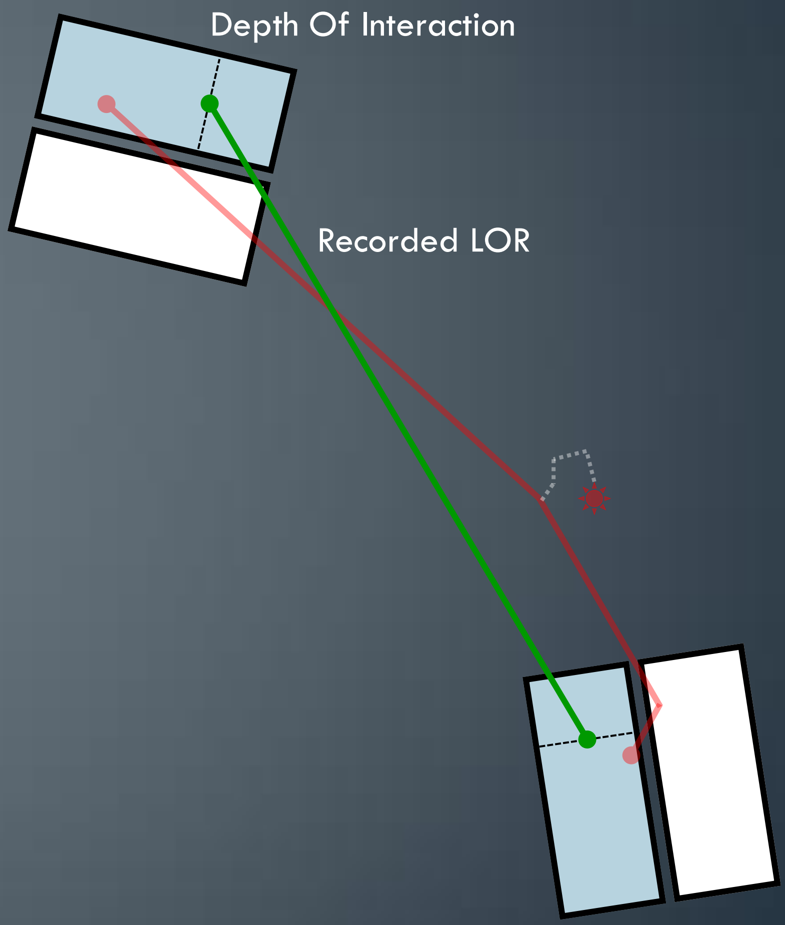

Positron range

Photon acollinearity

Detector response

Inter-crystal scatter

Crystal crosstalk

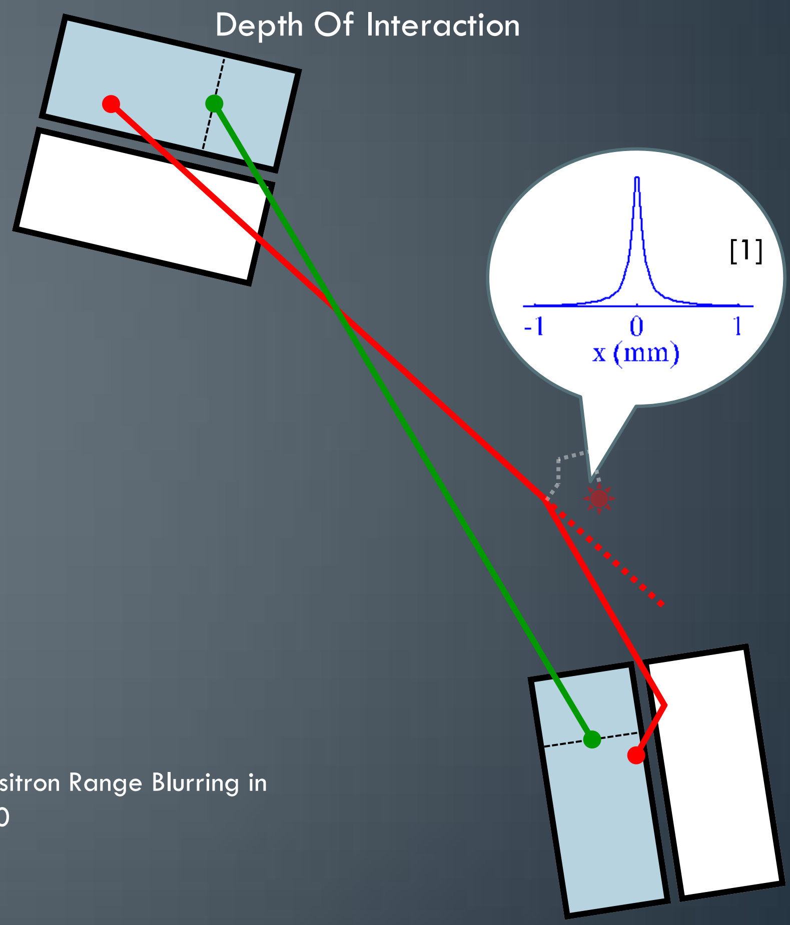

[1] Haber, S. F., *et al*, “Application of Mathematical Removal of Positron Range Blurring in Positron Emission Tomography”, *IEEE Trans. Nuc. Sci.*, 37:3, 1990

Positron range

Photon acollinearity

Detector response

Inter-crystal scatter

Crystal crosstalk

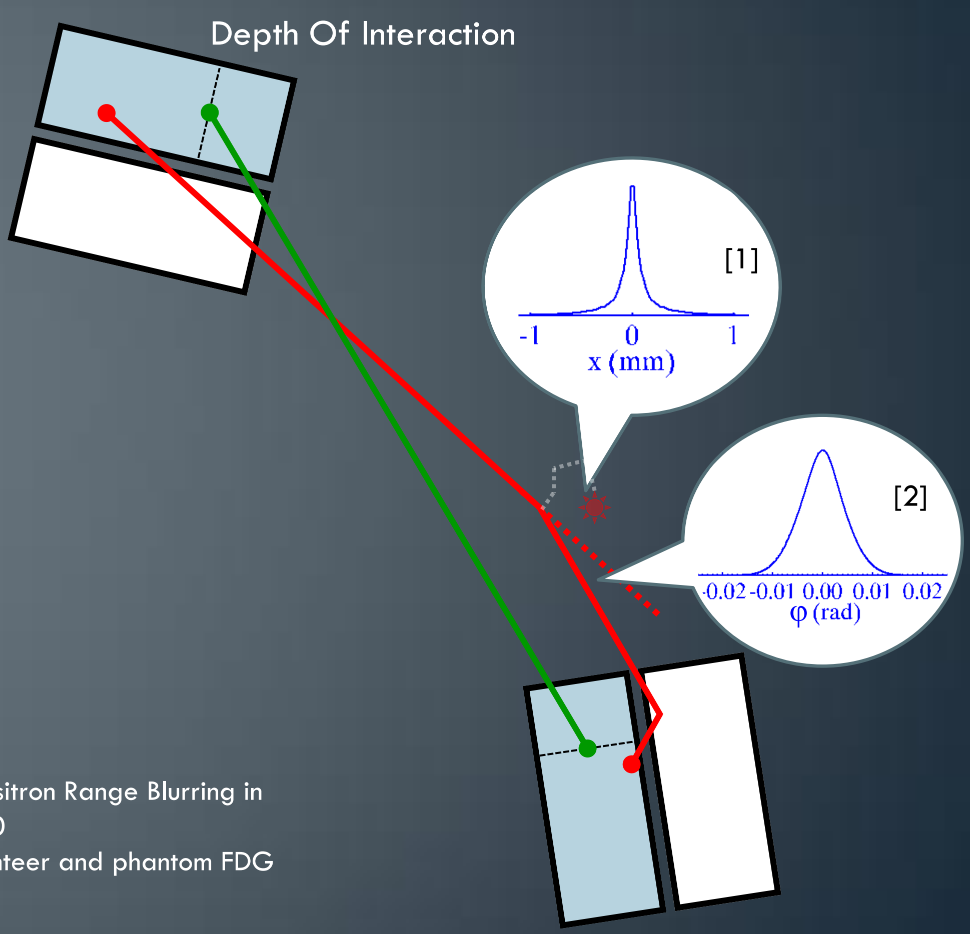

[1] Haber, S. F., *et al*, "Application of Mathematical Removal of Positron Range Blurring in Positron Emission Tomography", *IEEE Trans. Nuc. Sci.*, 37:3, 1990

[2] Shibuya, K., *et al*, "Annihilation photon acollinearity in PET: volunteer and phantom FDG studies", *Phys. Med. Biol.*, 52:17, 2007

Positron range

Photon acollinearity

Detector response

Inter-crystal scatter

Crystal crosstalk

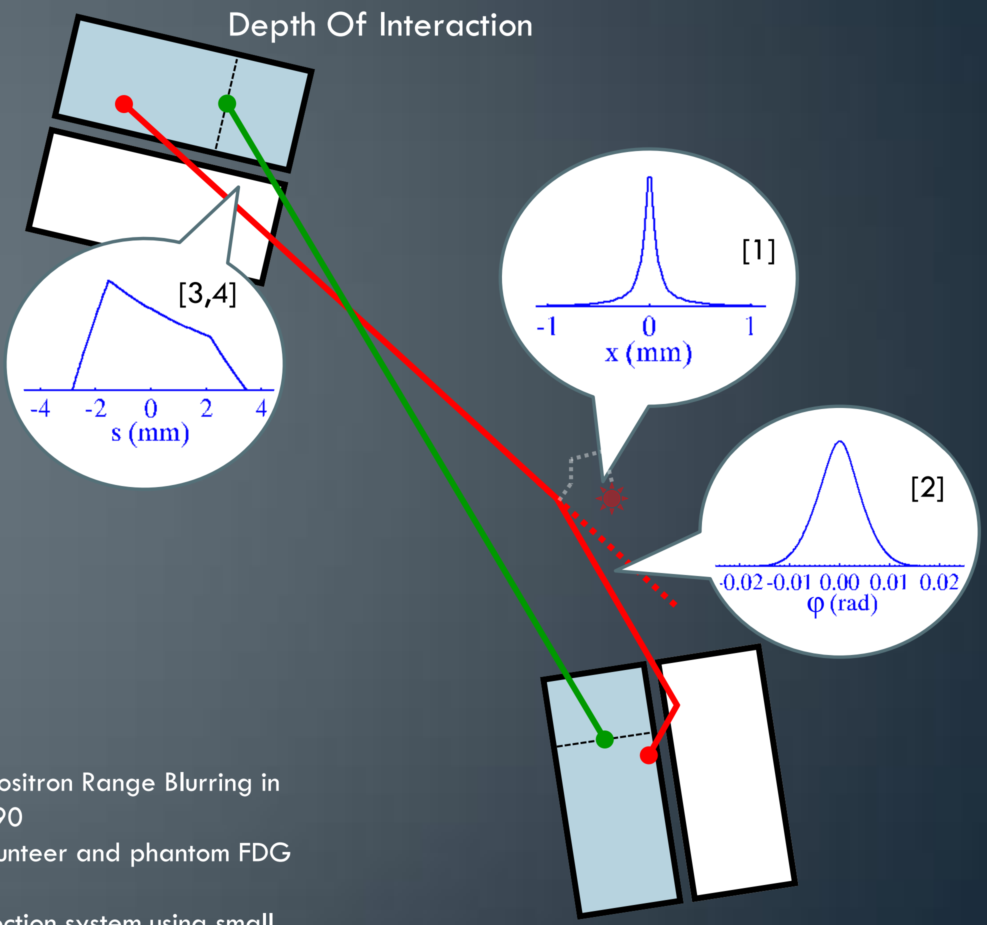

[1] Haber, S. F., *et al*, "Application of Mathematical Removal of Positron Range Blurring in Positron Emission Tomography", *IEEE Trans. Nuc. Sci.*, 37:3, 1990

[2] Shibuya, K., *et al*, "Annihilation photon acollinearity in PET: volunteer and phantom FDG studies", *Phys. Med. Biol.*, 52:17, 2007

[3] Lecomte, R., *et al*, "Geometric study of high resolution PET detection system using small detectors", *IEEE Trans. Nuc. Sci.*, 31:1, 1984

[4] Liang, Z., "Detector response restoration in image reconstruction of high resolution positron emission tomography", *IEEE Trans. Med. Imag.*, 13:2, 1994

Positron range

Photon acollinearity

Detector response

Inter-crystal scatter

Crystal crosstalk

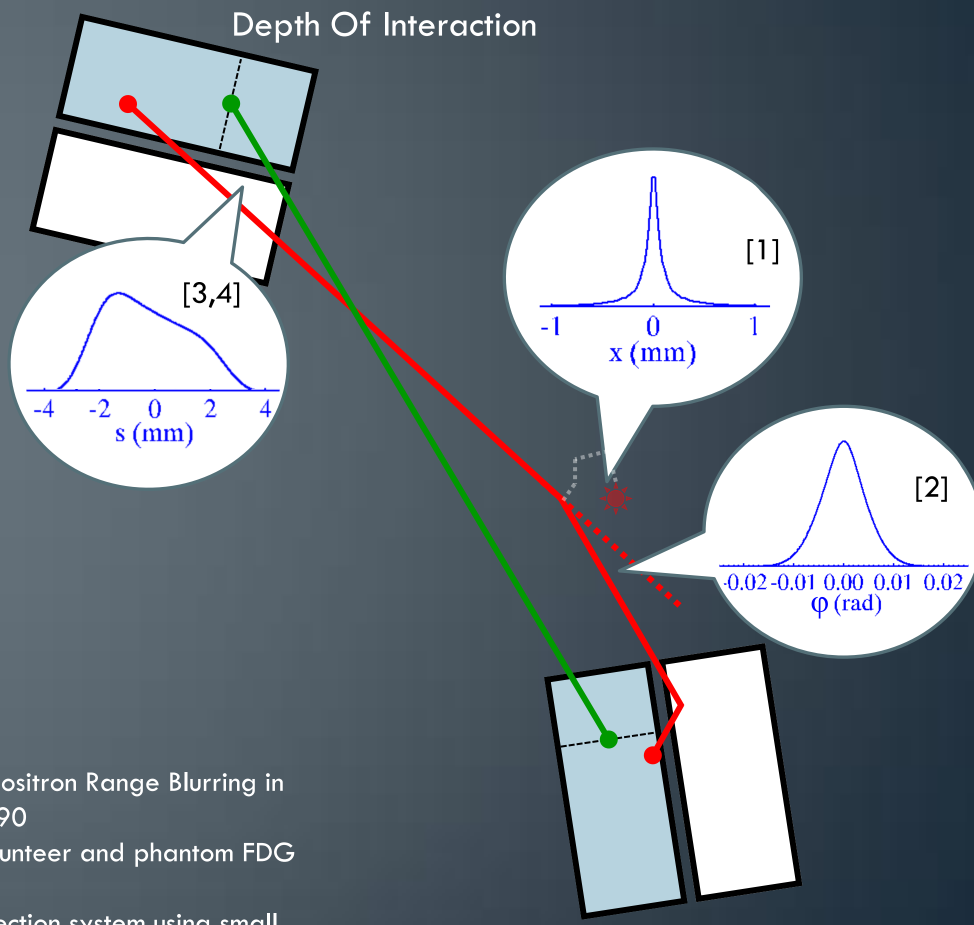

[1] Haber, S. F., *et al*, “Application of Mathematical Removal of Positron Range Blurring in Positron Emission Tomography”, *IEEE Trans. Nuc. Sci.*, 37:3, 1990

[2] Shibuya, K., *et al*, “Annihilation photon acollinearity in PET: volunteer and phantom FDG studies”, *Phys. Med. Biol.*, 52:17, 2007

[3] Lecomte, R., *et al*, “Geometric study of high resolution PET detection system using small detectors”, *IEEE Trans. Nuc. Sci.*, 31:1, 1984

[4] Liang, Z., “Detector response restoration in image reconstruction of high resolution positron emission tomography”, *IEEE Trans. Med. Imag.*, 13:2, 1994

Redistribute LORs accordingly

Many redistributed LORs create an effective tube-of-response

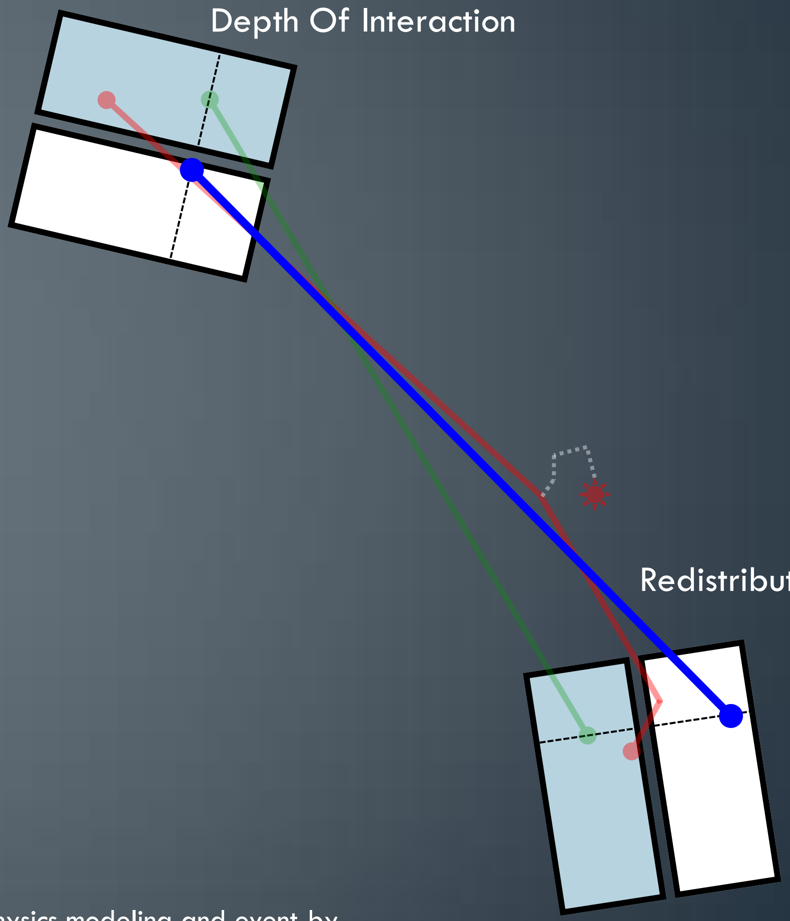

Jin, X., et al, “List-mode reconstruction for the Biograph mCT with physics modeling and event-by-event motion correction”, *Phys. Med. Biol, 58:16, 2013*

Gillam, J., *et* al, “Simulated one-pass list-mode: an approach to on-the-fly system matrix calculation”, *Phys. Med. Biol., 58:7, 2013*

The Distributions
Positron range convolution

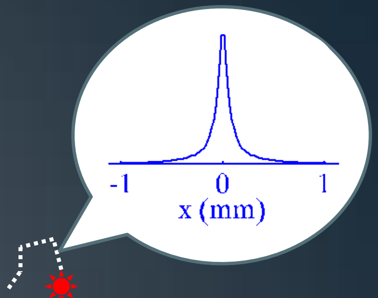

The positron range can be described by:

$$R(x) = Ae^{-x/B} + (1-A)e^{-x/C}$$ [1]

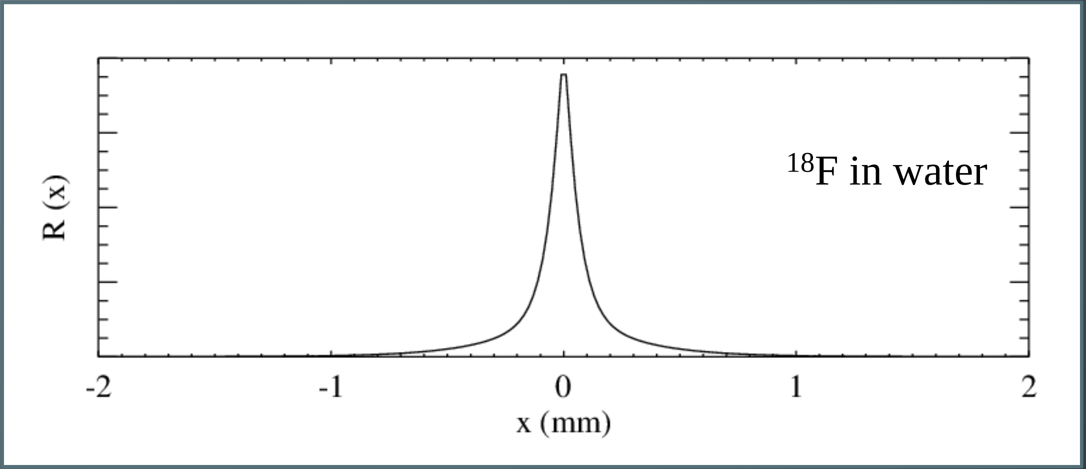

[1] Haber, S. F., *et al*, "Application of Mathematical Removal of Positron Range Blurring in Positron Emission Tomography", *IEEE Trans. Nuc. Sci.*, 37:3, 1990

The Distributions

Detector response function

$$P_\theta(s) = \left(1 - e^{-\mu_c y(s)}\right) e^{-\mu_c h(s) - \mu_g g(s)}$$ [1]

s	Length parameter orthogonal to LOR
$y(s)$	Path length through this crystal
$h(s)$	Path length through neighbouring crystal
$g(s)$	Path length through gaps
μ_c	Attenuation of crystals
μ_g	Attenuation of gap material ($BaSO_4$[2])

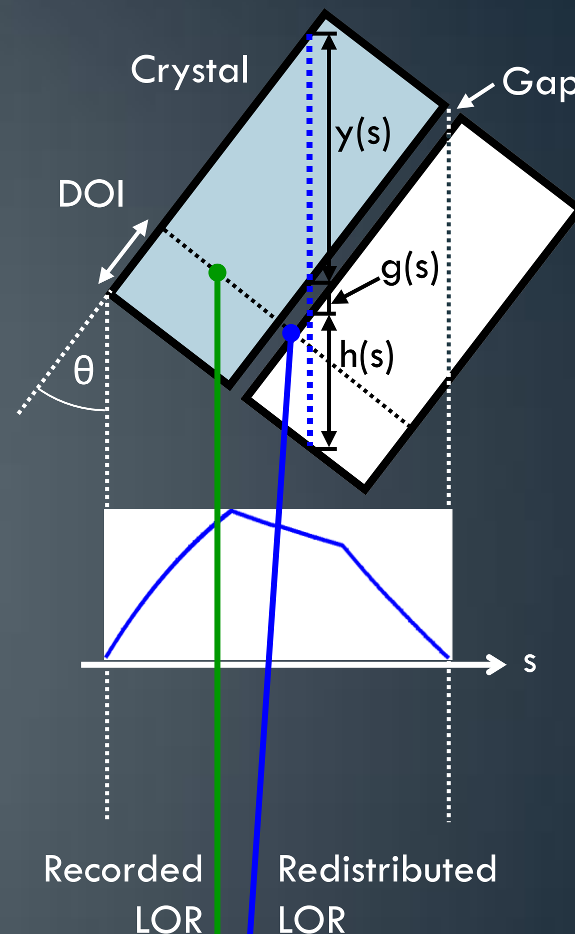

Crystal width = 1.510 mm
Transaxial gap width = 0.120 mm
Axial gap width = 0.082 mm

[1] Lecomte, R., *et al*, "Geometric study of high resolution PET detection system using small detectors", *IEEE Trans. Nuc. Sci.*, 31:1, 1984

[2] Tai, Y-C, *et al*, "MicroPET II: design, development and initial performance of an improved microPET scanner for small-animal imaging", *Phys. Med. Biol.*, 48, 2003

The Distributions

Detector response function

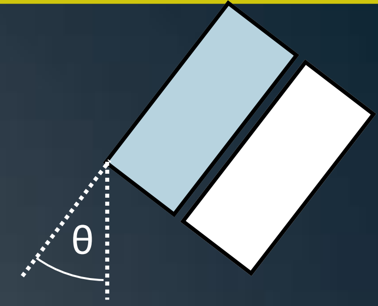

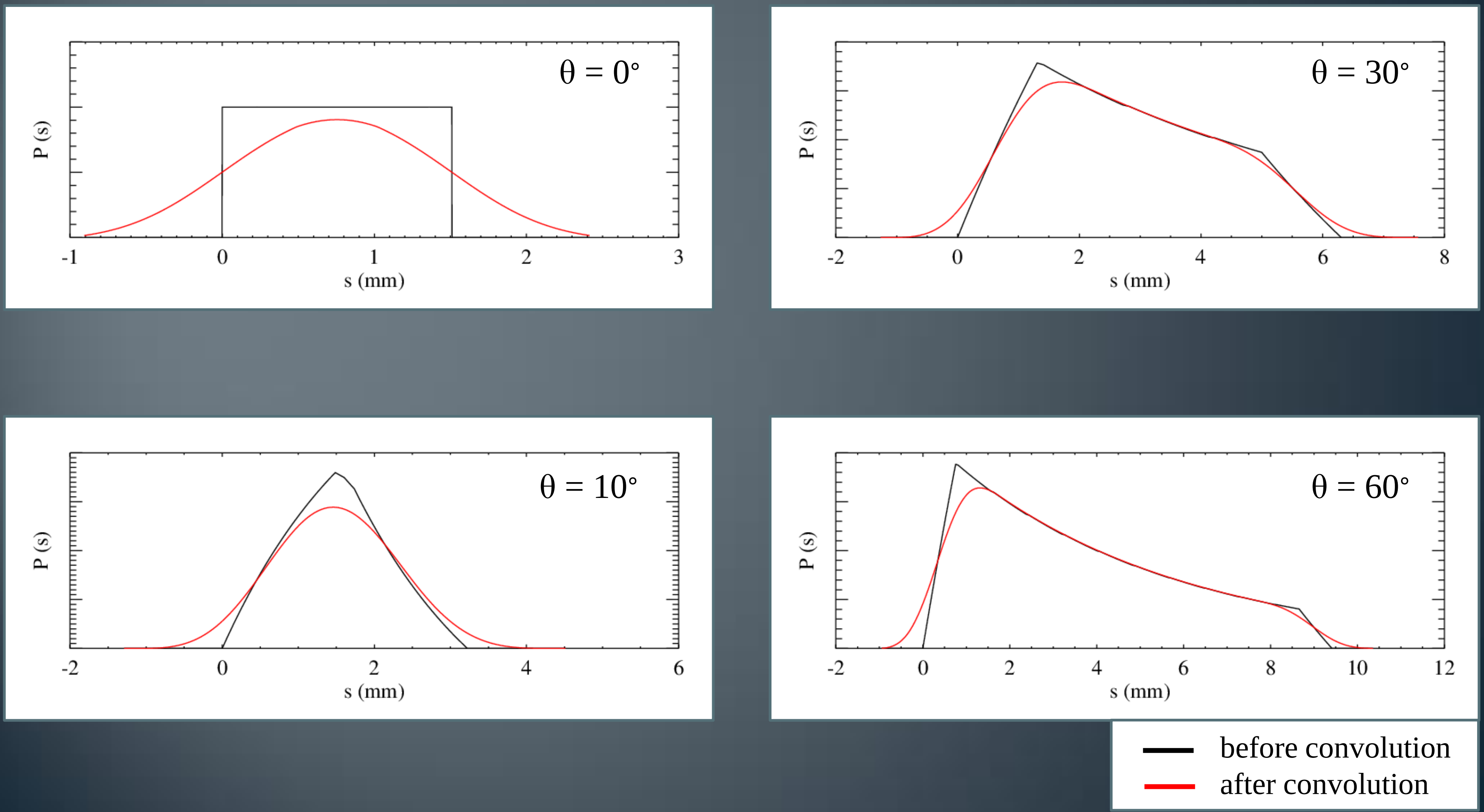

The Distributions

Acollinearity distribution

The angular deviation is best described by a double Gaussian:

$$Q(\phi) = A_1 e^{-\frac{(\phi-\mu_1)^2}{2\sigma_1^2}} + A_2 e^{-\frac{(\phi-\mu_2)^2}{2\sigma_2^2}}$$ [1]

A	0.824	0.176
μ (deg)	-0.009	0.007
σ (deg)	0.269	0.116

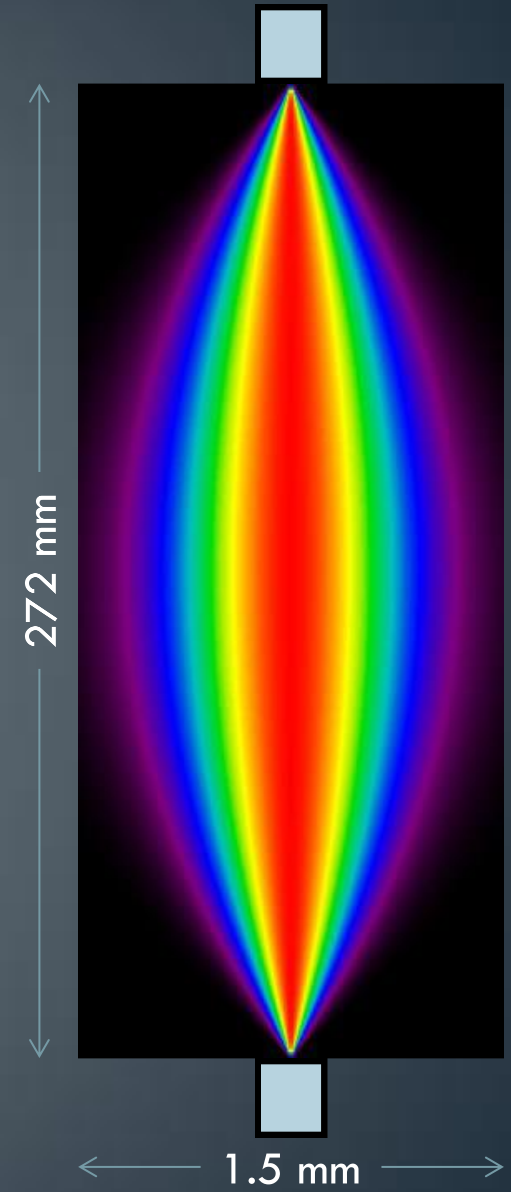

[1] Shibuya, K., *et al*, "Annihilation photon acollinearity in PET: volunteer and phantom FDG studies", *Phys. Med. Biol.*, 52:17, 2007

The Distributions

Acollinearity distribution

The LOR can be redistributed by either:

shifting one endpoint, or…

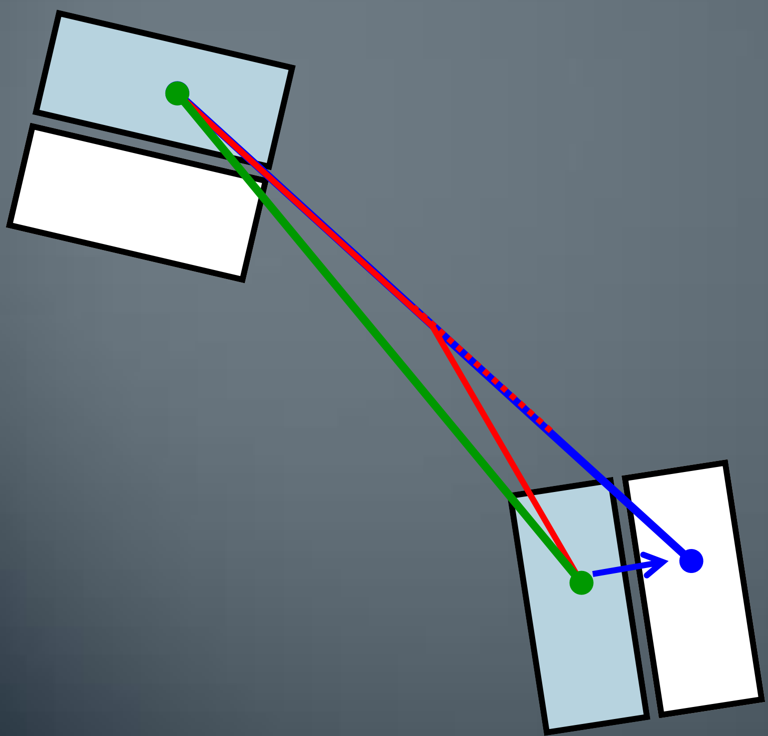

…shifting both endpoints

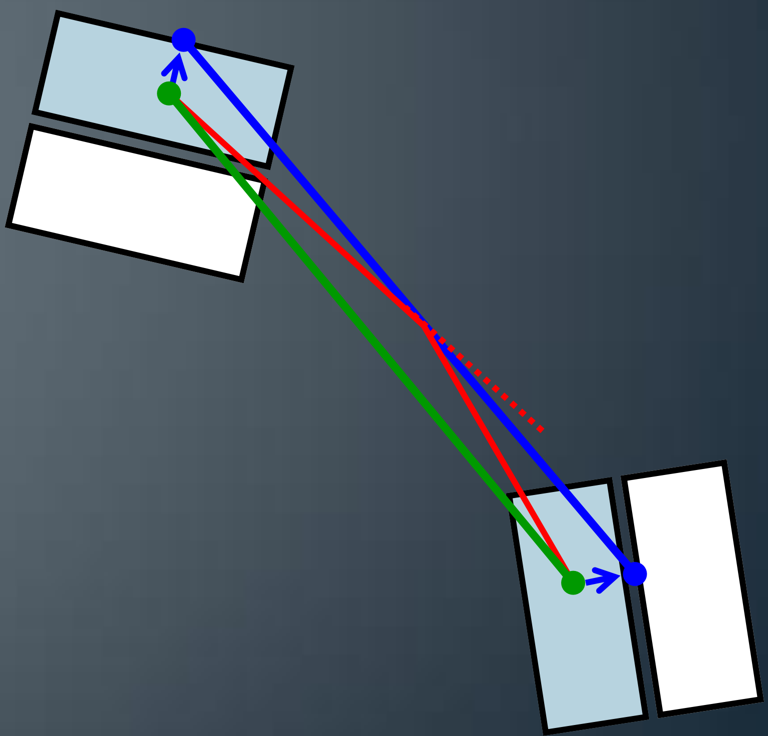

Theoretical distribution

The Distributions
Acollinearity distribution

The LOR can be redistributed by either:

shifting one endpoint, or…

…shifting both endpoints

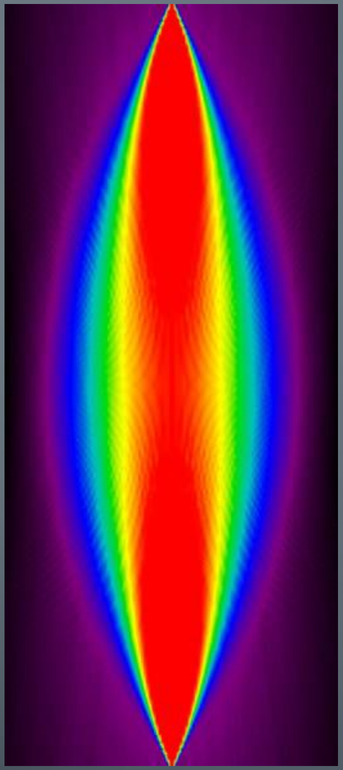

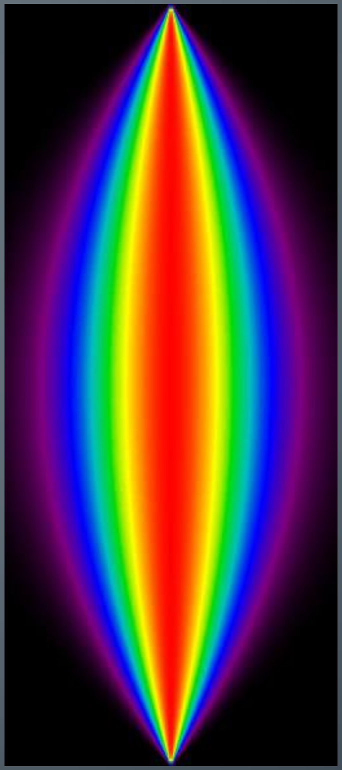

Theoretical distribution

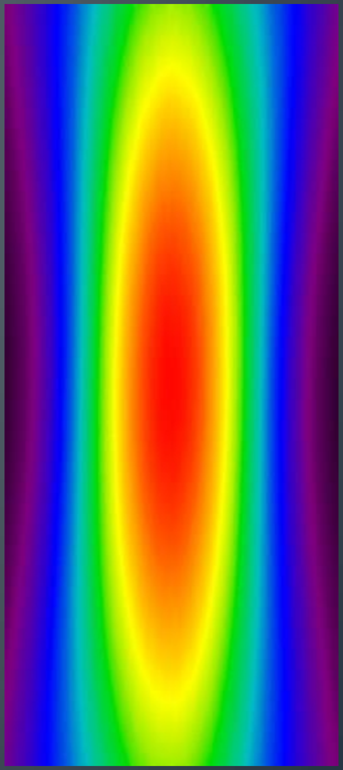

Implementation

1. LORs are redistributed twice, independently:

   once for forward projection and once for backprojection

2. List-mode MLEM reconstruction with subsets

3. LORs are resampled after every iteration

Spatial Variance

1. Point sources were measured
2. Point sources were simulated
3. Simulated point sources were forward projected:
    A. after convolution with a Gaussian, and,
    B. using redistributed LORs.
4. The sinogram profiles were compared

Spatial Variance

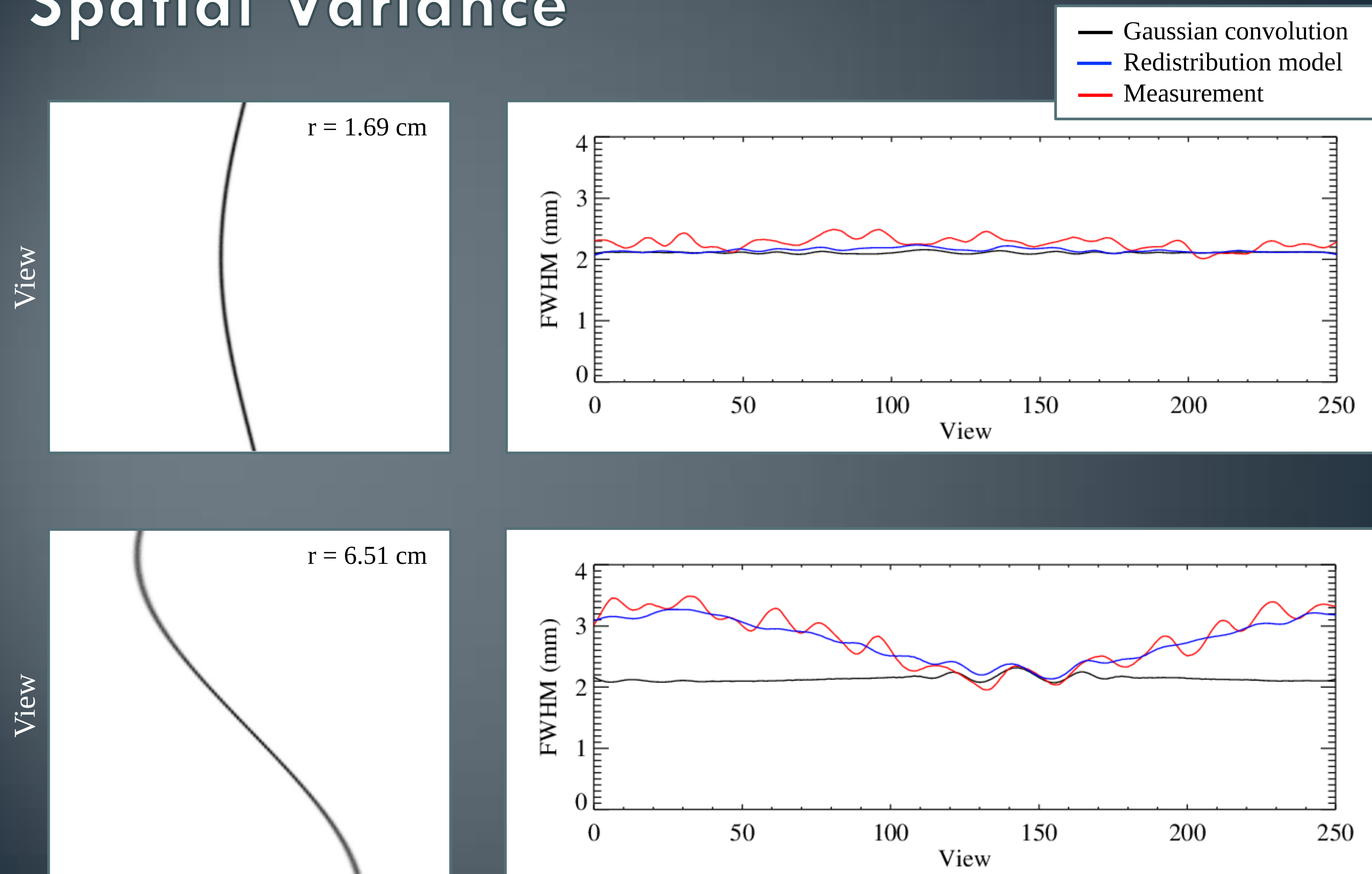

Phantom Reconstructions

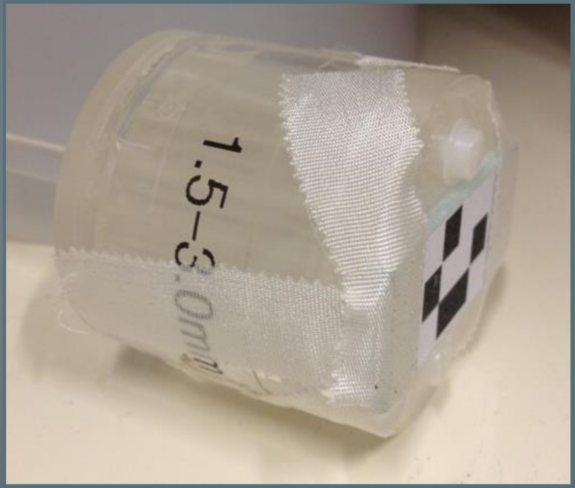

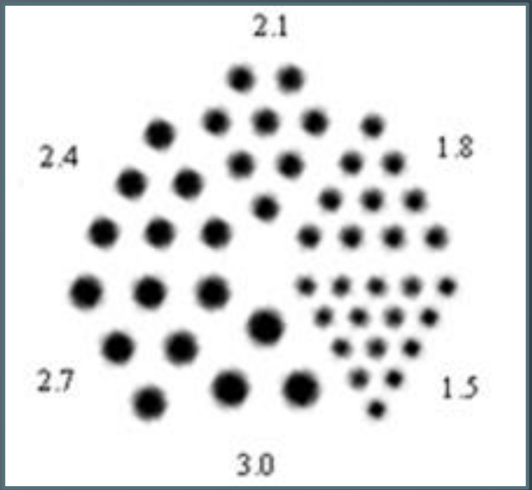

Phantom Reconstructions

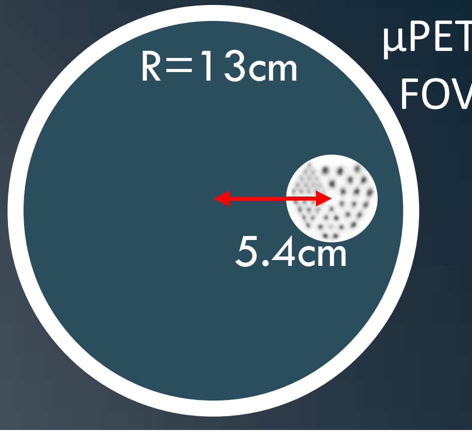

No resolution modelling

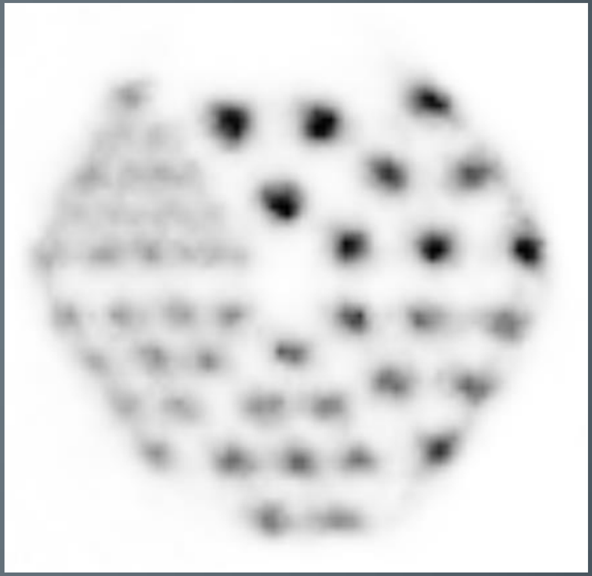

Redistribution

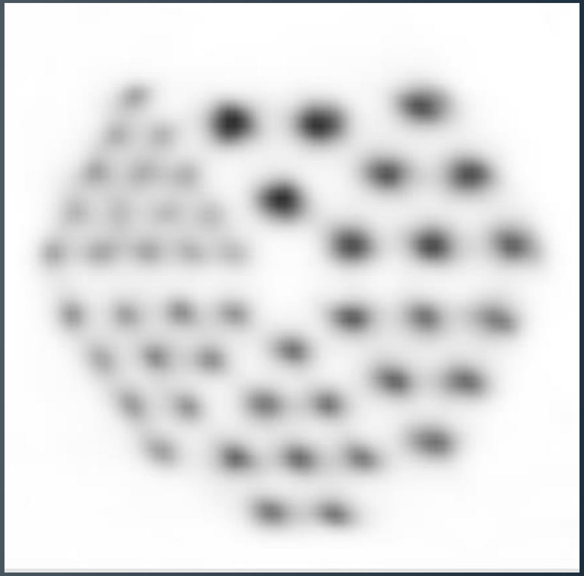

Gaussian convolution

Pixel: 0.4745 mm
10 Iterations , 10 subsets

Scan time: 5 minutes
Activity: 1.2 mCi of FDG
LORs: 150 million

Phantom Reconstructions

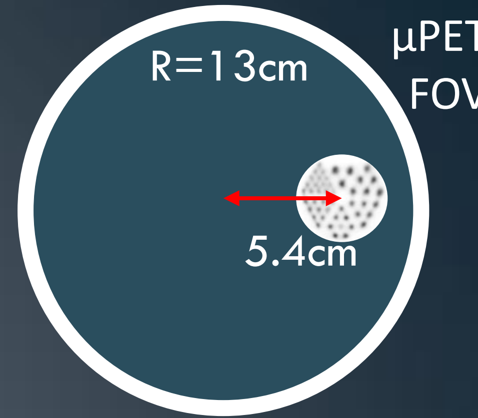

Summing 10
planes together

No resolution modelling

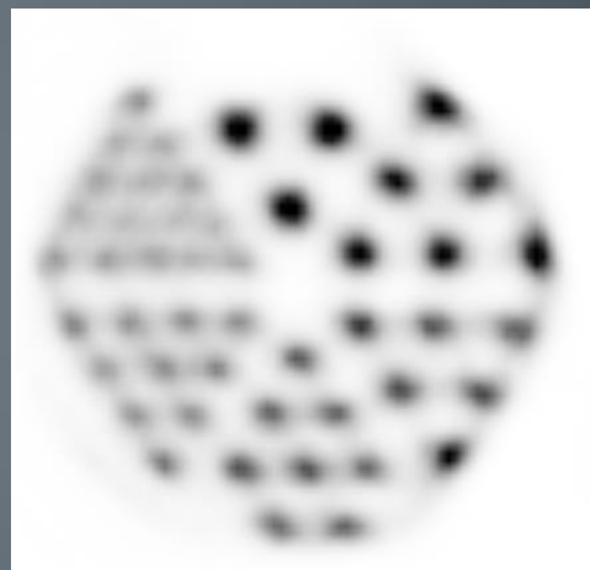

Redistribution

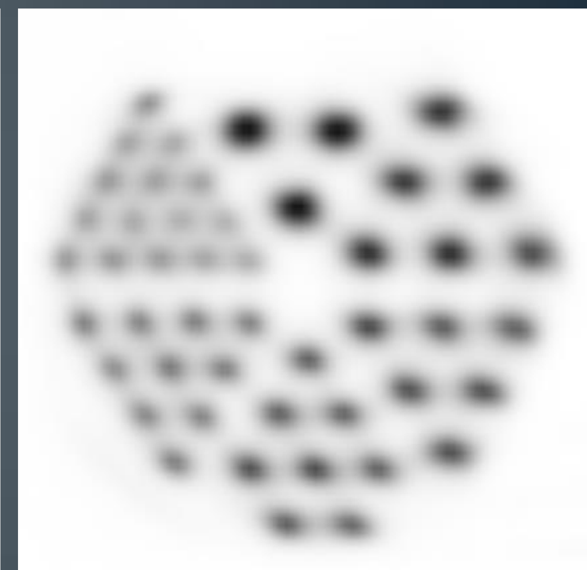

Gaussian convolution

Pixel: 0.4745 mm
10 Iterations , 10 subsets

Scan time:	5 minutes
Activity:	1.2 mCi of FDG
LORs:	150 million

Phantom Reconstructions

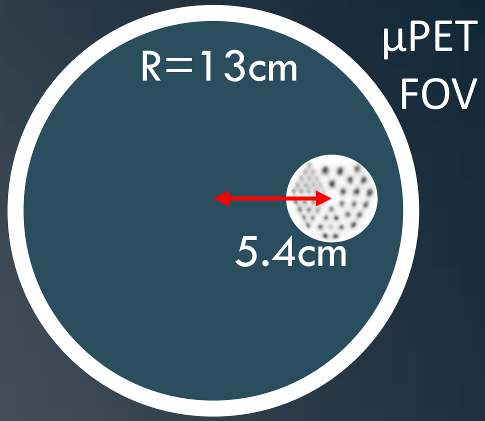

Summing 10
planes together

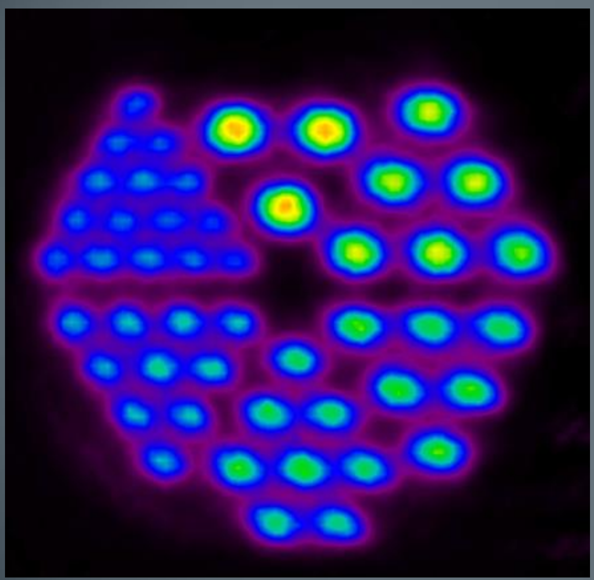

No resolution modelling

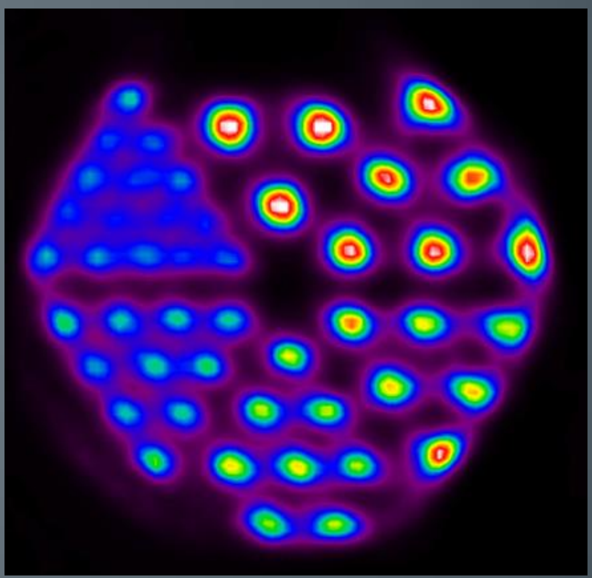

Redistribution

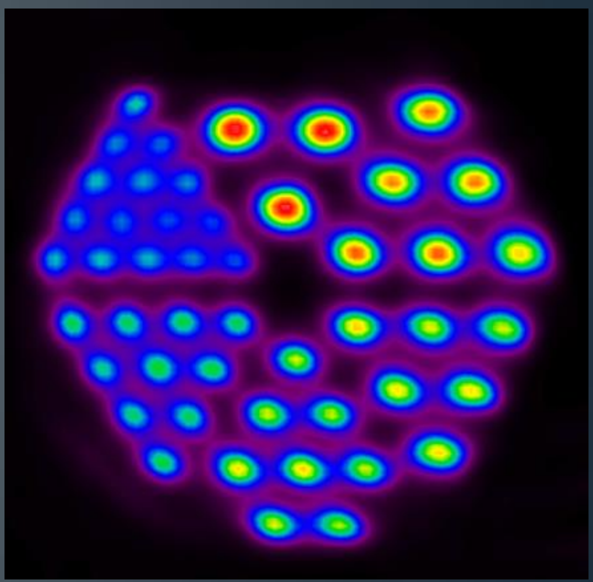

Gaussian convolution

Pixel: 0.4745 mm
10 Iterations , 10 subsets

Scan time: 5 minutes
Activity: 1.2 mCi of FDG
LORs: 150 million

Phantom Reconstructions

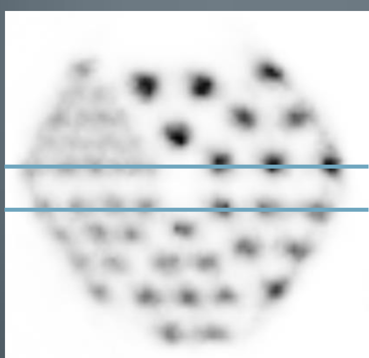

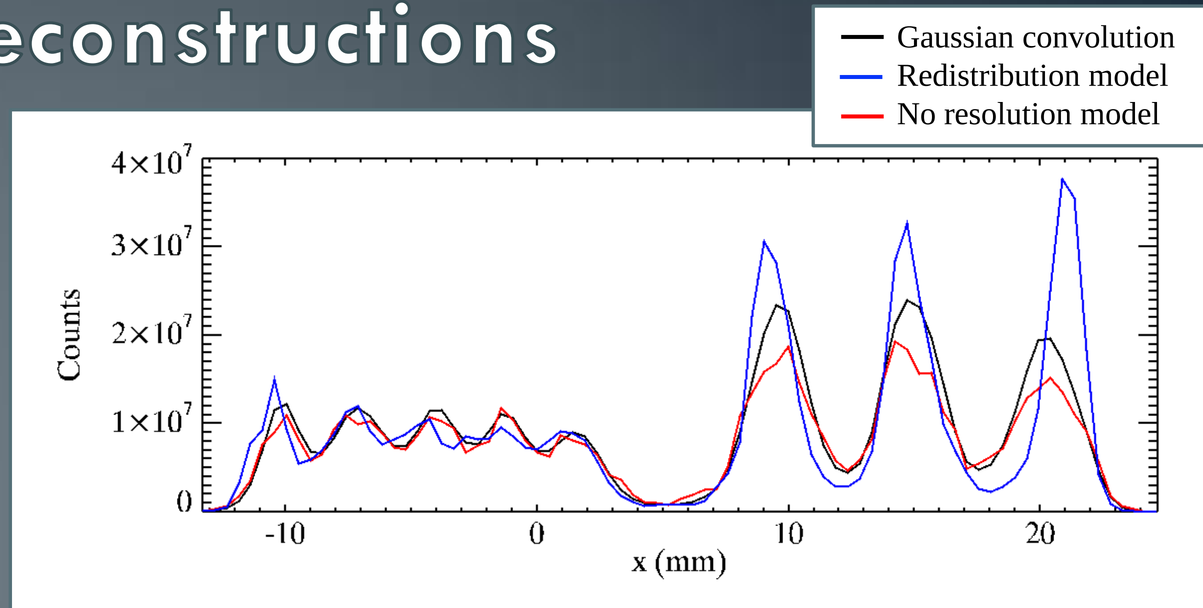

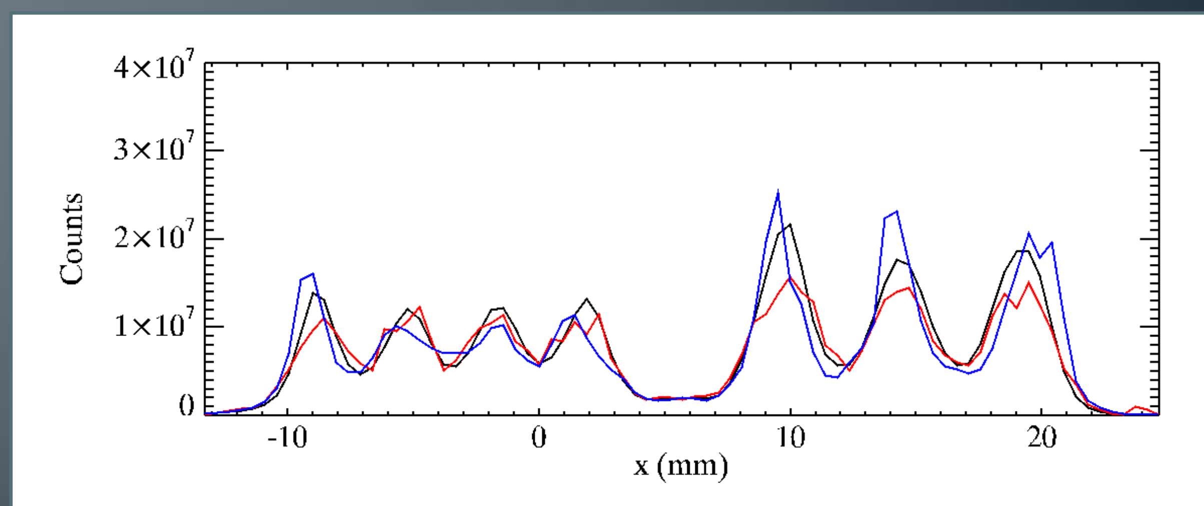

μPET
FOV

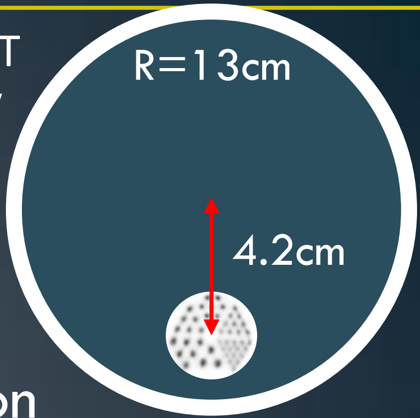

Combining models

Redistribution is used for forward and backprojection

Gaussian convolution is applied before forward and after backprojection

10 iterations

Standard
Gaussian convolution

Combined models

Pixel: 0.4745 mm

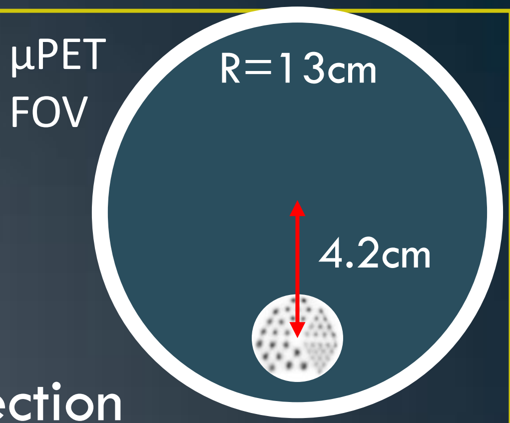

Combining models

Redistribution is used for forward and backprojection

Gaussian convolution is applied before forward and after backprojection

20 iterations

Standard
Gaussian convolution

Combined models

Pixel: 0.4745 mm

μPET
FOV

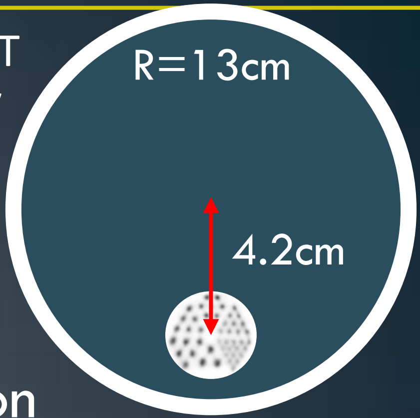

Combining models

Redistribution is used for forward and backprojection

Gaussian convolution is applied before forward and after backprojection

20 iterations

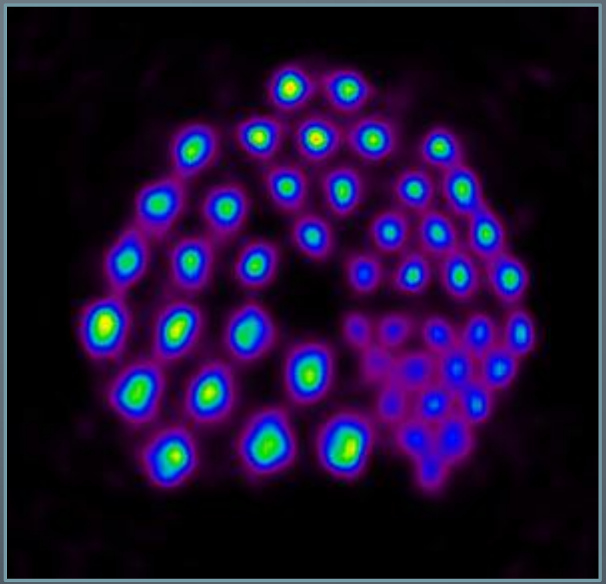

Standard
Gaussian convolution

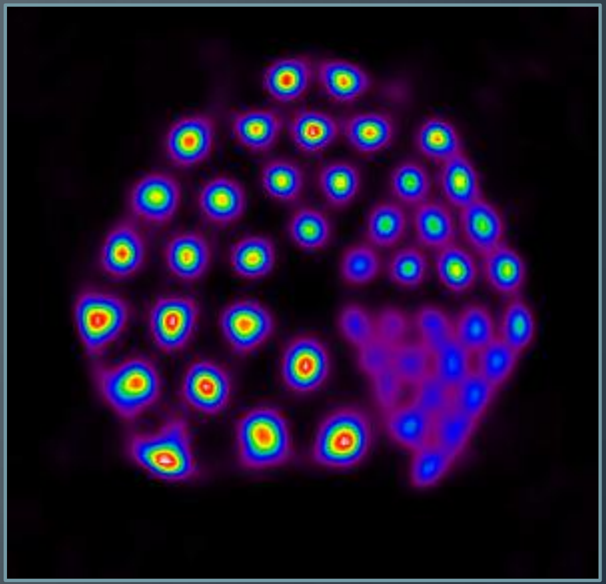

Combined models

Pixel: 0.4745 mm

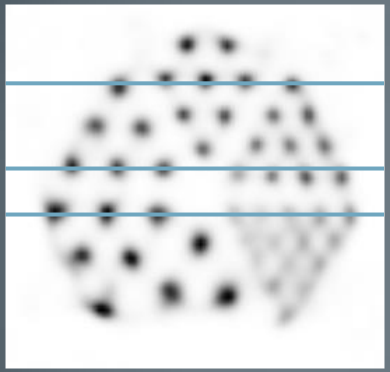

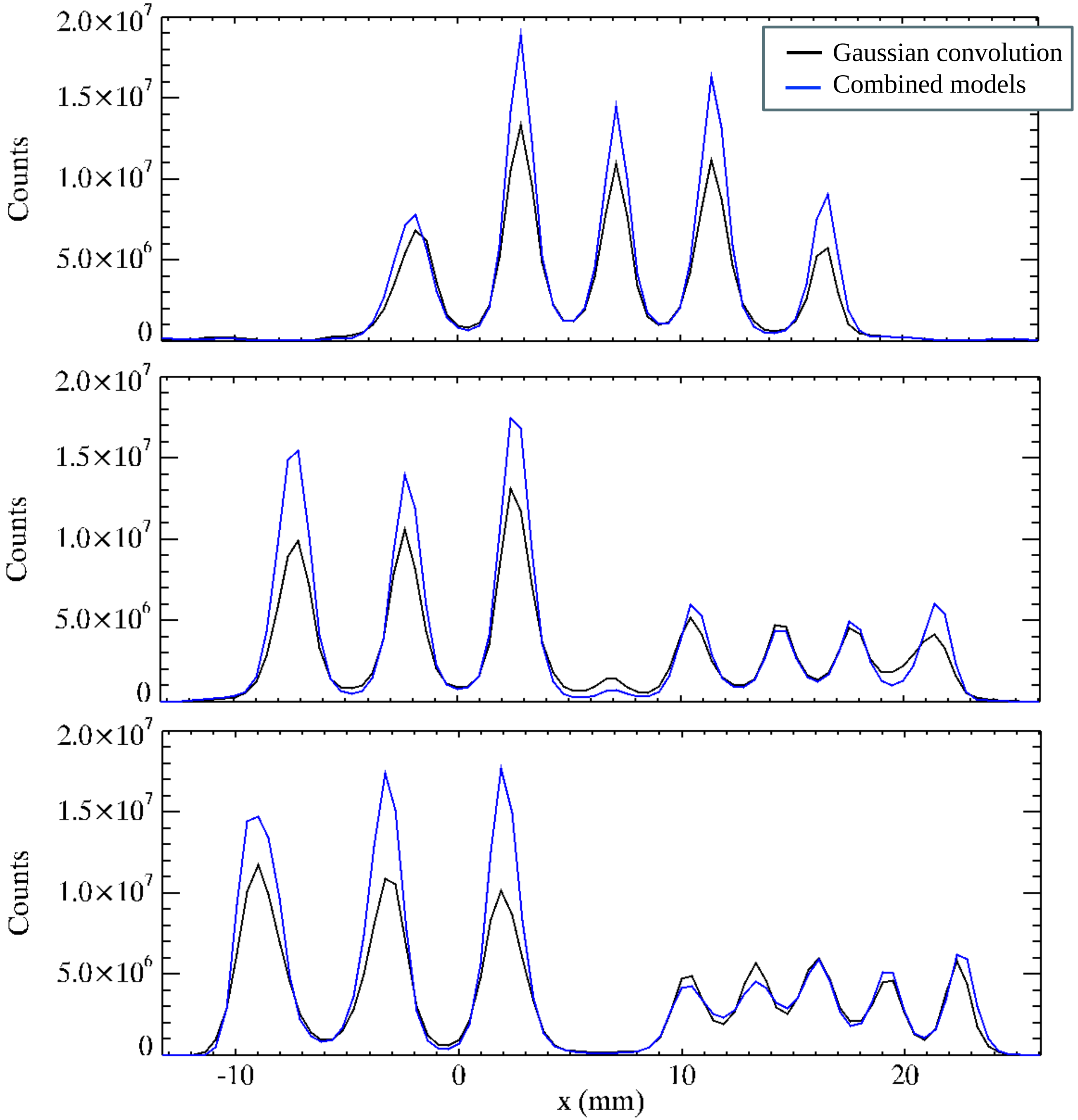

Gaussian convolution
Combined models
Counts
2.0×10^7
1.5×10^7
1.0×10^7
5.0×10^6
0
-10
0
10
20
x (mm)

Motion correction

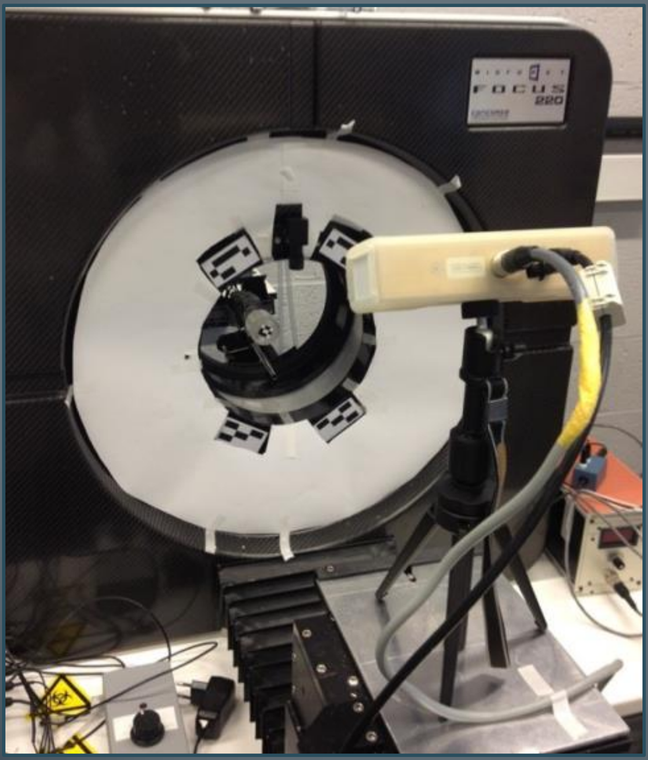

Brain imaging of fully awake, tube-bound rat

Motion data recorded by MicronTracker stereo-optical camera

List-mode data corrected after acquisition and before reconstruction

Motion correction

With redistribution:

- The LORs are redistributed before being motion corrected
- Spatial variance of the model is preserved correctly

Motion correction

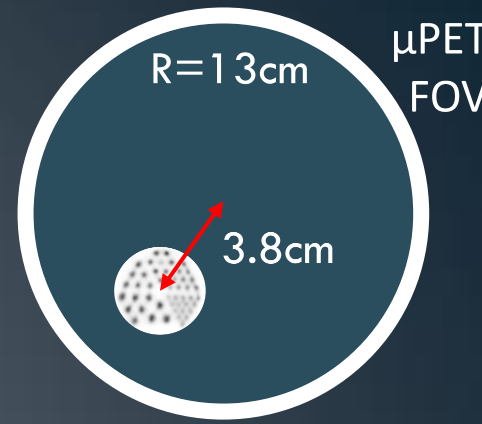

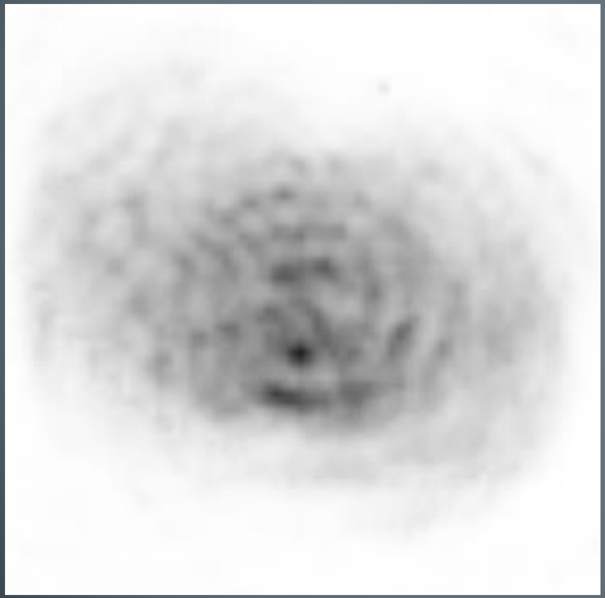

Not motion corrected

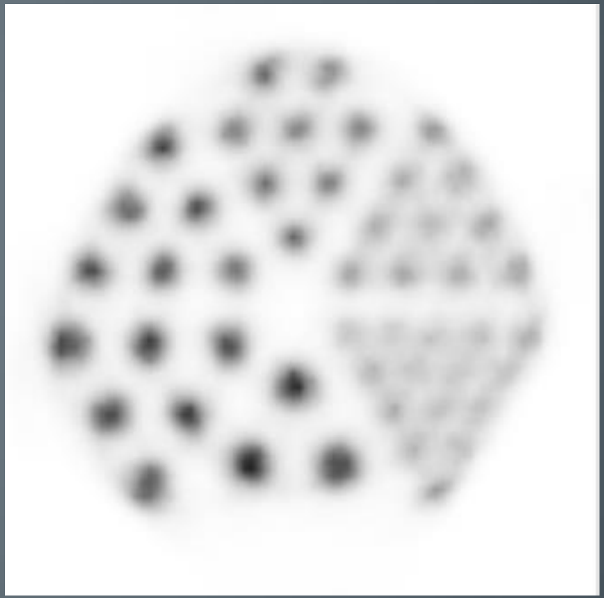

Redistribution

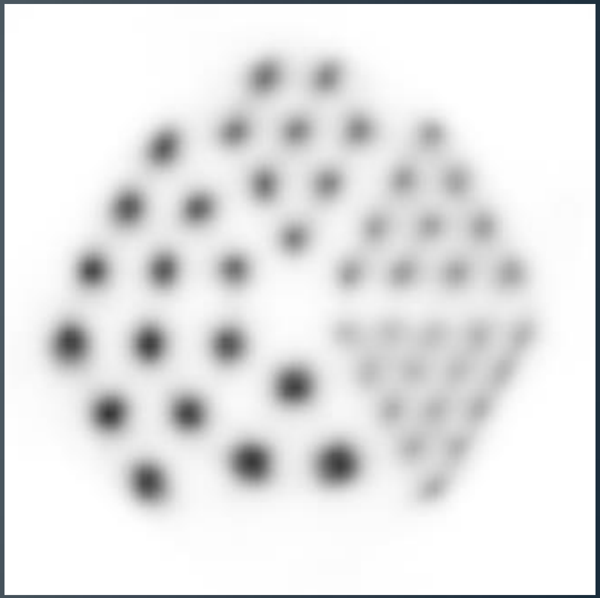

Gaussian convolution

Pixel: 0.4745 mm
10 iterations, 10 subsets

Scan time: 5 minutes
Activity: 1 mCi of FDG
LORs: 130 million

Motion correction

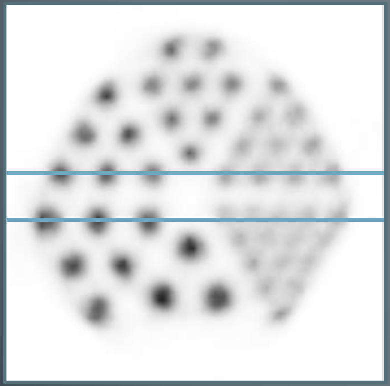

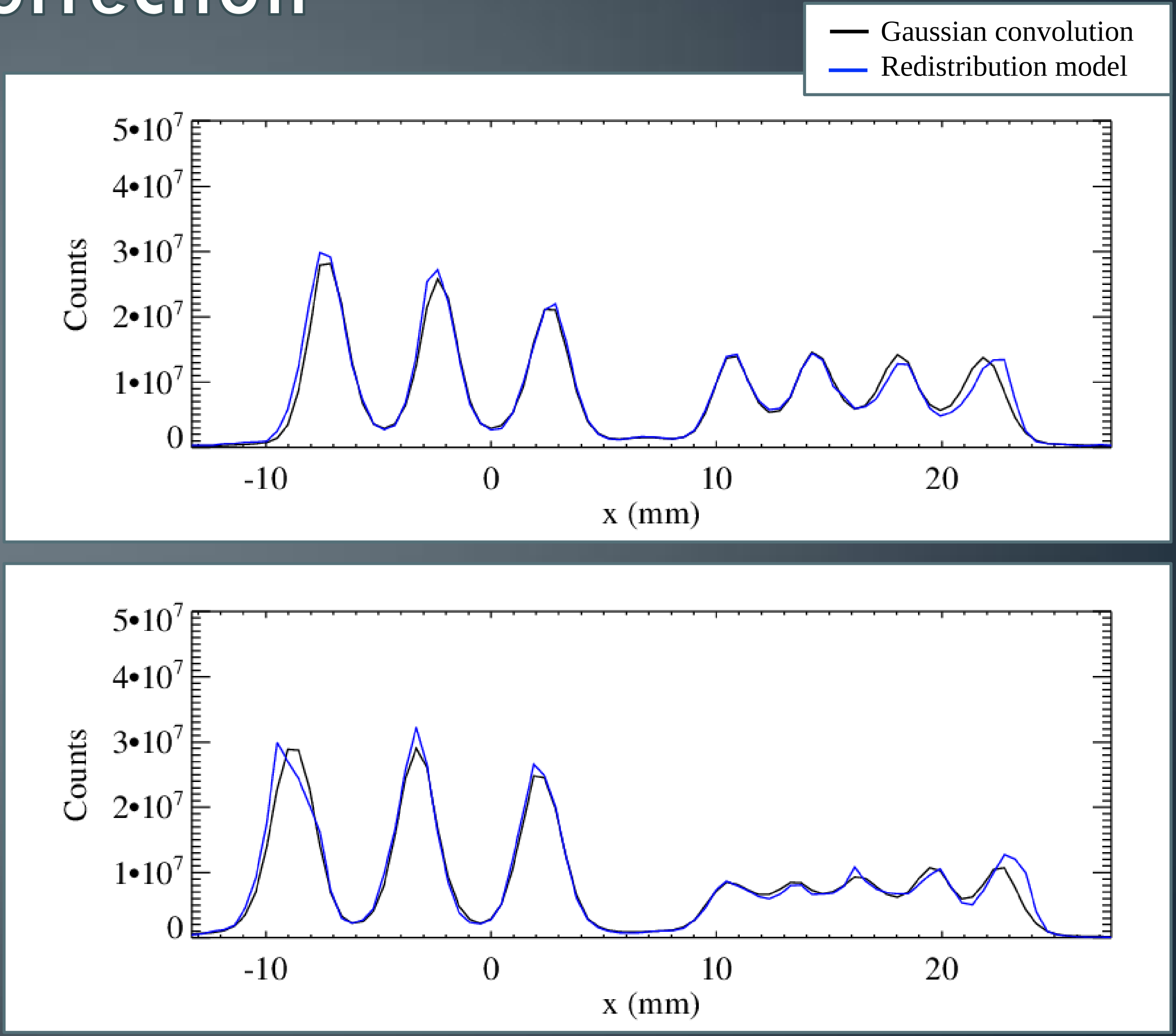

Conclusion

- A spatially variant resolution modelling technique has been introduced
- LORs are randomly redistributed accordingly to probabilistic system response functions
- System matrix is computed on-the-fly
- Easily applicable to list-mode rigid motion correction

- Shows improvement in off-centre resolution
- Noise propagation needs to be suppressed

Motion correction

No motion

When the rat moves, assume microPET moves rather than rat

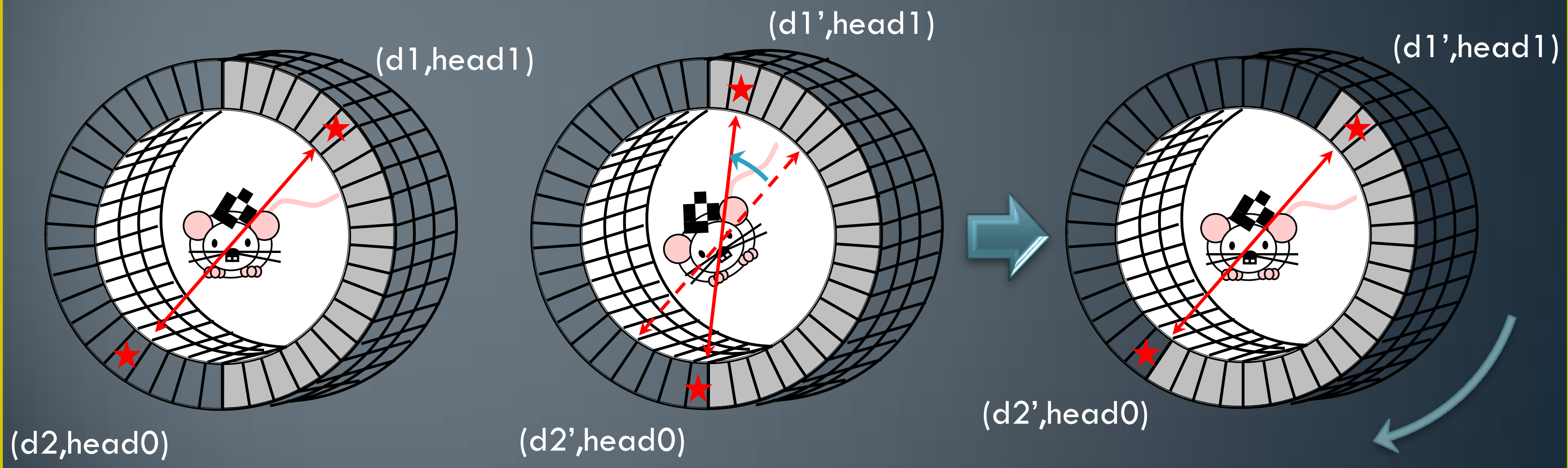

Change of LOR orientation due to motion estimated by MicronTracker

Motion correction

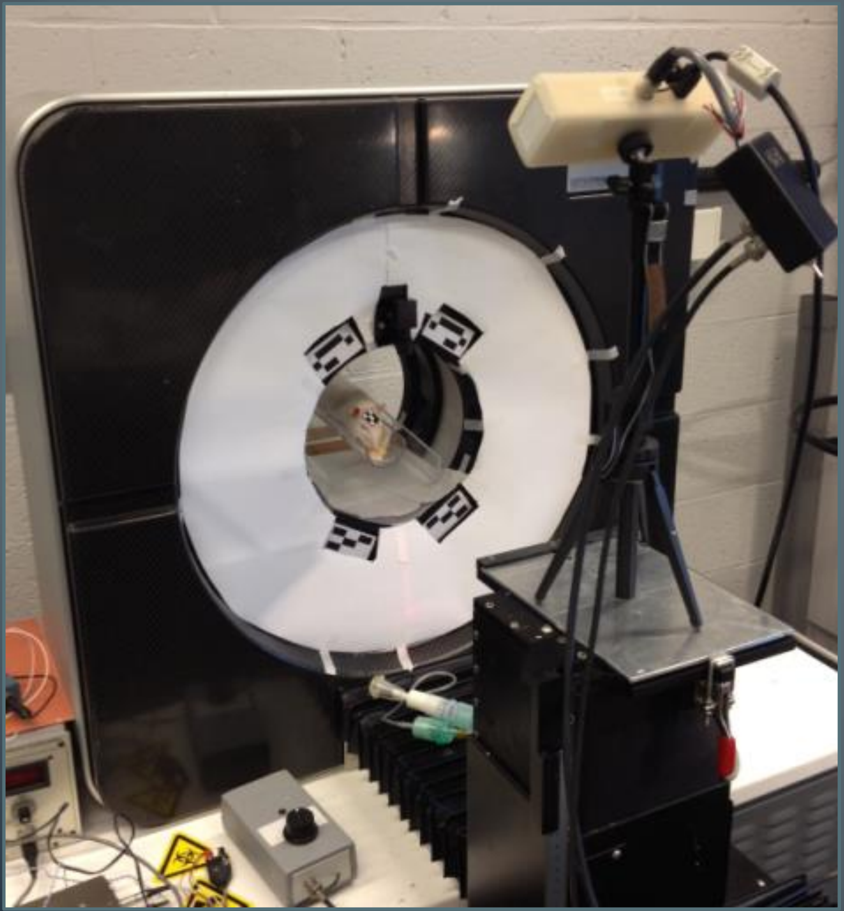

Motion scan:
15 minutes
60 min post injection

Static scan:
20 minutes
85 min post injection